Organic and Medicinal Chemistry
International Journal
ISSN 2474-7610

Research Article
Volume 10 Issue 2 - November 2020
DOI: 10.19080/OMCIJ.2020.09.555782

Organic & Medicinal Chem IJ

A New Approach to Design Hydroxyapatite and Silk Fibroin Bone Substitutes

Daniela Vieira[1,2]*, Dayane Dotto[1], Eliana C da S Rigo[1], Sheyla M C M Bicalho[3] and Sergio A Yoshioka[1]

[1]*Graduate Program in Bioengineering, University of São Paulo, Brazil*

[2]*Experimental Surgery, Faculty of Medicine, McGill University, Canada*

[3]*JHS Biomateriais, Brazil*

Submission: October 13, 2020; **Published:** November 25, 2020

***Corresponding author:** Daniela Vieira, Graduate Program in Bioengineering, University of São Paulo, São Carlos 13566-590, Brazil

Abstract

Biomaterials to regenerate bone have been gaining great visibility in tissue engineering. The design of a material like bone is a great challenge, especially when combining the ideal mechanical strength, porosity, and bioactivity. This work focused on the development of a new candidate for bone substitute combining hydroxyapatite (HAp) and silk fibroin (SF). The silk fibroin, obtained from the cocoons of the silkworm (Bombyx mori), was dissolved using a ternary solution of calcium, ethanol, and water. HAp was co-precipitated dropping phosphate solution (Na2HPO4) in SF at a constant stirring. The final composite, 75%HAp/25%SF, were framed using a hydraulic system varying the pressure to find the best candidate. Physical and chemical characterizations were evaluated, as well as the bioactivity and cytotoxicity. Results showed excellent chemical and physical properties, like the trabecular bone. The 75%HAp/25%SF biocomposite was safe to CHO cells and presented great bioactivity being an alternative candidate to the bone regeneration field.

Keywords: Hydroxyapatite; Silk fibroin; Co-precipitation; Bone scaffold; Tissue engineering

Introduction

Tissue engineering is a promising strategy for the field of bone regeneration. Only in 2020, approximately 6.6 million of orthopedic surgeries were performed worldwide due to the bone fractures, disease, or malformation. As the world population grows at a fast rate, there is a huge need on developing substitutes able to mimic the structure and function of the original bone [1-3]. The current focus on bone substitute is on bioactive materials, where the material can interact to biological molecules and cells, and, simultaneously, regenerating the bone tissue. The ideal material for bone regeneration should present osteoconduction, osteoinduction and osteointegration; as well as good mechanical strength, porosity, and biocompatibility [2,4,5].

Hydroxyapatite (HAp) has been attracting a lot of attention as bone substitute biomaterial because of high porosity and three-dimensional porous structure, which provide optimal conditions for the growth and proliferation of cells. Furthermore, its porosity allows oxygen and nutrients diffusion, creating vascular integration. However, HAp is naturally fragile making it not suitable to be framed by itself [2,3,5]. To increase the mechanical properties of HAp different strategies have been applied, as such as the incorporation of natural polymers (collagen, chitosan, and silk fibroin). Silk fibroin (SF), has been widely used in the biomedical field due to excellent biocompatibility and mechanical properties, in addition, it presents excellent thermodynamic properties (degradation>150°C) when compared to the available biopolymers, such as collagen [6,7].

Current, there are several research combining HAp and SF in different proposals, such as gel, sponges, cements, etc. However, the current methodologies involve expensive and time-consuming techniques and cannot reach the perfect balance between mechanical strength and porosity [8]. Here we designed a simple and cost-effectiveness strategy able to create HAp/SF scaffolds with ideal porosity and mechanical strength.

Materials and Methods

All chemicals were obtained from Sigma. Silk fibroin solution was prepared following Ajisawa protocol [9]. Briefly, 5g of Bombyx mori silkworm cocoons (donated by Bratac, Brazil) were degummed for 30 minutes in a boiling 0.02M sodium carbonate solution to remove sericin. The degummed silk was rinsed 3 times in deionized water and dried overnight at 45°C. The dried silk fibers were dissolved in a 0.1M $CaCl_2$/0.2M ethanol/0.8M H_2O

solution at 70°C for 4h. The final silk fibroin solution was filtered (MF-Millipore™ MCE Membrane Filters – Sigma) to remove impurities. We designed a co-precipitation technique to prepare HAp/SF composites. Briefly, we prepared a solution containing 0.12 mol of Na_2HPO_4 in 150mL of 0.5M Tris-HCl solution at pH 9.0. The concentration of phosphate was proportional to Ca concentration to obtain 1.67 ratio of Ca/P. The final solution was slowly dropped into the silk fibroin solution with intense mechanical stirring (10,000 RPM) for 30 minutes. To obtain the best candidate, different ratios of HAp/SF were studied (65/35%, 75/25%, 85/15% e 95/5%). The best candidate was molded using a hydraulic system (Prensa MAXX – 3ton, Essence Dental) using a circular stainless frame (Ø9mm x10mm) and dried at 60°C for 48h. Two different pressures (50 MPa and 100 MPa) were studied to get the desired mechanical resistance and porosity characteristic. Finally, the molded composite was washed in distillated water for 48h (changing water every 4h) and dried at 60°C for 48h.

Physical and chemical characterizations

SEM images were obtained in a ZEISS LEO 440 (Cambridge, England) equipment with OXFORD detector (model 7060), operating with 20 kV electron beam, 2.82A current and 200pA I probe. The samples were coated with carbon using Coating System BAL-TEC MED 020 (BAL-TEC, Liechtenstein). Pores size were measured from SEM images using ImageJ software. EDX was performed on Isis System Series 200 equipment, with SiLi Pentafet detector, ATW II ultra-thin window (ATW II) window, from 133eV to 5.9keV, coupled to a LEO Electron Microscopy Ltd), using an Oxford Detector (Oxford Instruments Inc.). Thermogravimetric analyze (TGA) was performed from 25°C to 800ºC, in a synthetic air, using 10 mg at heating rate of 10ºC.min-1 (Q-50 model - TA Instruments). FTIR spectra were performed using A Shimadzu IRAffinity-1 spectrophotometer, with 64 scans and resolution of 4 cm^{-1}, wave range from 400 to 4000 cm^{-1} on KBr tablets.

X-ray diffraction was applied to verify crystallinity using a Bruker D8 Discovery Instrument X-ray diffratometer (CuKa radiation, 2θ diffraction). Mechanical compression was performed using a TIME GROUP 30 KN equipment, with load cells of 5-ton, speed of 0.5 mm/minute. The total porosity was calculated based on the Archimedes method (NBR ISO 5017:2015) [10]. Briefly, samples were dried at 60°C for 24h. After dried, samples were weighted and recorded as M1. Samples were then placed in a beaker containing ethanol. Deaeration cycles were applied to complete absorption of ethanol inside the samples. After complete ethanol immersion, the weight was measured and recorded as M2. Finally, the immersed sample was weighted and recorded (M3) using mechanical analytical balance. The % of liquid absorption (%LA) was calculated using equation I and the % of apparent porosity (%AP) using equation II.

$$\%LA = \frac{M2 - M1}{M2} \times 100 \quad (1)$$

$$\%AP = \frac{M2 - M1}{M2 - M3} \times 100 \quad (2)$$

Micro computed tomography (micro-CT) was applied to observe the composite in 3D images, evaluating its volume, porosity, and pore connectivity. The samples were scanted in SkyScan 1172 Micro-CT equipment (SkyScan; Kontich, Belgium). The reconstruction of the images was performed using NRecon (Version 1.6.2.0; SkyScan). Ct-Vol software (SkyScan, August 2003, Aartselaar, Belgium) was used to calculate porosity and volume.

In vitro analyses

Cytotoxicity was performed in CHO cells using neutral red assay (ISO 10993-5 - Test for *in vitro* cytotoxicity) [11]. Phenol was used as a positive control (toxic) and alumina as a negative control (non-toxic). The bioactivity was evaluate based on the apatite formation using ISO 23317 protocol [12]. Briefly, samples were incubated in SBF solution at 36.5°C for 0, 14 and 28 days. After incubated period, SEM was performed to verify visually the apatite formation.

Results and Discussion

Physical and chemical characterizations

The porosity, mechanical strength and ratio of calcium/phosphate are essential parameters to analyze the performance of a bone substitute [13-15]. Here, to assure the best ratio of hydroxyapatite (HAp) and silk fibroin (SF), we pre-analyzed these parameters for different ceramic/polymer ratio after manually framed to find the best candidate for the study. We concluded that the 75% HAp/25%SF presented more favorable performance when compared to other proportions investigated (Table 1). In this way, the hydraulic pressing procedure and others characterization were evaluated on 75%HAp/25% SF ratio.

Table 1: Pre-test to evaluate the best candidate for the study.

Sample	Ca/P ratio	% Liquid Absorption (g/g)	Compressive Strength (MPa)
65%HAp+35%SF	1.89 ± 0.01	63.8 ± 2.2	0.25 ± 0.11
75%HAp+25%SF	1.67 ± 0.15	61.4 ± 0.8	0.36 ± 0.01
85%HAp+15%SF	2.23 ± 0.23	58.8 ± 1.5	0.11 ± 0.05

The interconnection and distribution of pores are fundamental to allow cells adherence, proliferation, and differentiation. In addition, it provides paths to nutrients and oxygen flows, helping with the growth of the new tissue and blood vessels [15,16]. The SEM images in Figure 1 show the 75%HAp/25%SF composite morphology.

How to cite this article: Daniela V, Dayane D, Eliana C d S R, Sheyla M C M B, Sergio A Y. A New Approach to Design Hydroxyapatite and Silk Fibroin Bone Substitutes. Organic & Medicinal Chem IJ. 2020; 10(2): 555782. DOI: 10.19080/OMCIJ.2020.09.555782

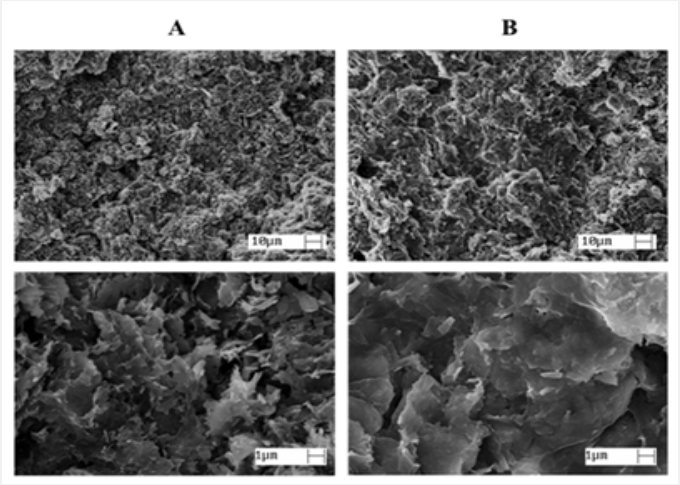

Figure 1: The interconnection and distribution of pores for 75% HAp/25%SF composites pressured at (A) 50 MPa and (B) 100 MPa.

A similar pore distribution was observed for samples pressed at 50 MPa and 100 MPa, presenting diameters between 1µm and 50µm. The composite had a homogeneous and well-interconnect structure. The co-precipitation procedure allowed a well bound between HAp and SF, especially due to the carbonyl group present in SF that binds to the Ca+2, that forms carbonyl-calcium complexes. When dropping the phosphate solution, PO43- accumulated around the complex and initiated the nucleation of HAp. Due to the strong chemical interaction between the carbonyl groups and Ca2+, SF induced the self-organization and orientation of HAp crystals. Finally, HAp is cross-linked with the SF, forming this homogeneous network [17-19]. EDX analysis showed the Ca/P ratio of 1.67, like the inorganic bone material [20] (Figure 2).

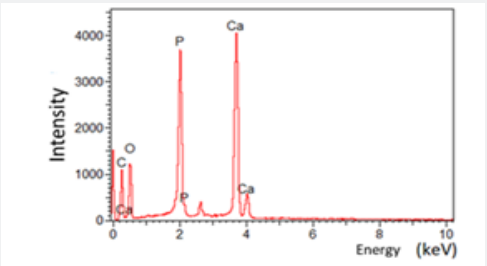

Element	Experimental (%)	Theory*[20] (%)
C	27.27	0
O	39.73	59.09
P	12.39	13.64
Ca	20.61	22.73
H	N/A	4.54
Ca/P	1.67	1.67

Figure 2: EDX analysis for 75%HAp/25%SF composite.

The thermo behavior of 75% HAp/25%SF is shown in Figure 3A. We observed the water evaporation between 25°C and 120°C. The SF degradation started around 290°C when it is alone and shifted to 300°C when it is bound to HAp, indicating the strong link between SF and HAp [13,18,20,21]. The total weight loss was 35%, where 5% was related to the water evaporation, showing that the organic/inorganic composition is approximately 70/30, close to the desired ratio 75/25.

How to cite this article: Daniela V, Dayane D, Eliana C d S R, Sheyla M C M B, Sergio A Y. A New Approach to Design Hydroxyapatite and Silk Fibroin Bone Substitutes. Organic & Medicinal Chem IJ. 2020; 10(2): 555782. DOI: 10.19080/OMCIJ.2020.09.555782

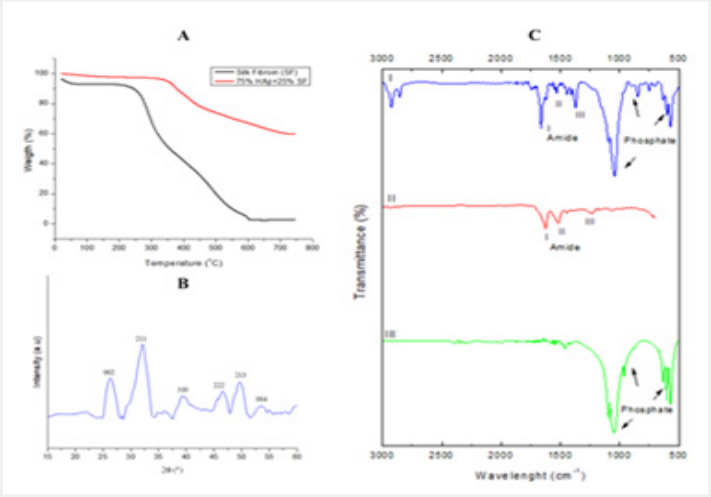

Figure 3: (A) TGA, (B) XRD and (C) FTIR of 75% HAp/25% SF composite.

FTIR studies were applied to analyze the structure based on the functional groups. Figure 3B shows the spectra of the

i. 75%HAp/25%SF,

ii. silk fibroin and

iii. deproteinized bone (donated by biochemistry and biomaterials group of IQSC- USP/Brazil).

The absorption bands at 1098, 1041, 844, 601 and 568 cm^{-1} are related to PO4-3 present in HAp

(i). Similar bands were identified in the deproteinized bone (ii) because of the vibrations of phosphate ion [22-24]. The bands at 1658, 1532 is 1368 cm^{-1} are characteristics of vibrations of the I, II, III amide groups, respectively, present in silk fibroin (i and ii). It is important to note a more intense peak for 75%HAp+25%FS compared to the silk fibroin, indicating an increase in β-conformation due to the link with HAp [25-27].

XRD spectrum for 75%HAp/25%SF is shown in Figure 3C. The crystallographic plans at (002), (211), (310), (222), (213) and (004) represent the characteristic pattern of HAp, showing no formation of any different calcium phosphate. However, these peaks are broaded and overlapped (evidenced in the 211 plan) demonstrating the presence of amorphous phase in HAp precipitated, very similar to biological apatite present in natural bone [28,29]. The HAp crystallinity is directly affected by the temperature; low temperature process creates broaded peaks and amorphous phases, while at higher temperatures, the peaks are sharper, indicating an increase in the crystallinity. Similar results were found in different studies with HAp/SF composites. Different works observed the overlapping at (211) plan, resulting in low crystallinity and more amorphous phase compared to HAp synthetic [13,17,18,30].

The % of porosity and % of liquid absorption of 75%HAp / 25% SF is described in Table 2. The ideal porosity of a bone substitute must be greater than 30% to allow interconnection and provide sufficient opportunities for cell migration and proliferation [5,14,15]. Through the liquid absorption capacity, it is possible to preview if the material will be able to guarantee the diffusion process for cells, nutrients, and oxygen [14,15]. Similar % of apparent porosity and % of liquid absorption were found for samples pressed at 50MPa and 100MPa. Samples pressed at 100 MPa presented an increase of ~5% for these parameters compared to samples pressed at 50 MPa. Both samples presented great structure to allow cells adherence and growth, with porosity above 50%.

Table 2: The porosity of 75%HAp/25%SF shows a great ability to allow the flow of cells, nutrients, and oxygen.

75%HAp/25%SF	Apparent Porosity (%)	Liquid Absorption (%)
50 MPa	52.23 ± 2.15	34.31 ± 2.51
100 MPa	56.83 ± 2.20	40.89 ± 5.16

One of the greatest challenges on the development of bone substitutes is combine the ideal porosity and mechanical resistance. A structure with the ideal porosity often sacrifices the mechanical properties and vice-versa. Mechanical compression tests were performed to evaluate the stress behavior of 75% HAp/ 25% SF pressed at 50 and 100 MPa (Figure 4). The samples pressed at 50 MPa and 100 MPa showed compressive stress of 2.62±0.74 and 2.13±0.16 MPa, respectively, like the trabecular bone. Our composite demonstrated sufficient strength to ensure the early stabilization right after implant, supporting the first

How to cite this article: Daniela V, Dayane D, Eliana C d S R, Sheyla M C M B, Sergio A Y. A New Approach to Design Hydroxyapatite and Silk Fibroin Bone Substitutes. Organic & Medicinal Chem IJ. 2020; 10(2): 555782. DOI: 10.19080/OMCIJ.2020.09.555782

compressive stress. Usually, the scaffolds for bone substitutes are made using hydraulic pressing or freeze-drying methodology. The first process guarantees a higher compressive strength, sacrificing the porosity, while the second one, ensure a good porosity but decrease its strength. Different works involving HAp and SF observed a significant increase in the mechanical strength when SF was incorporated to the material [13,15,31-33].

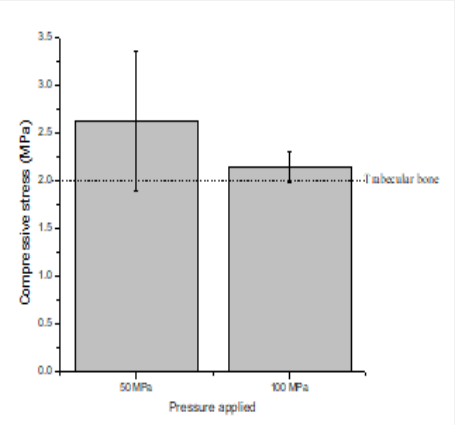

Figure 4: Compressive strength response in function of pressure applied, 50 and 100MPa, respectively. The 75%HAp/25%SF composite demonstrated similar behavior to trabecular bone.

Another way to verify the interconnection of pores could be applying images techniques such as micro computed tomography (micro-CT). Figure 5 shows 3D images of 75%HAp/25%SF composite pressed at (a) 50MPa and (b) 100MPa. The complete analysis is in Supporting information Table 3. Here, according to the analyses carried out by SEM, we could observe porous from 1µm to 50µm, where most pores are ~35 µm but not exceeding 50µm. This pore size distribution allows the flow of osteocytes, osteoclasts, and the growth of blood vessels.

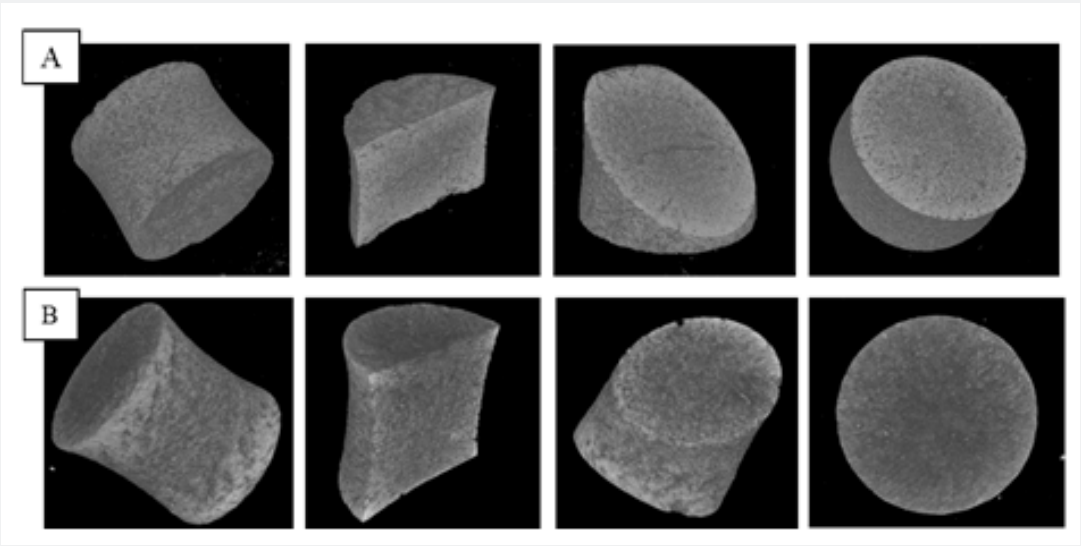

Figure 5: Micro-CT 3D images showing a homogenous morphology for 75%HAp/25%SF pressed at (A) 50 MPa and (B) 100 MPA.

Table 3: CTvol analyses for 75%HAp/25%SF composite pressed at 50MPa and 100MPa

(75%HAp/25%SF)	50 MPa	100 MPa
Total volume (mm^3)	404,12	570,45
Filled volume (mm^3)	368,19	542,32
Porosity – closed porous (%)	8,89	4,93

How to cite this article: Daniela V, Dayane D, Eliana C d S R, Sheyla M C M B, Sergio A Y. A New Approach to Design Hydroxyapatite and Silk Fibroin Bone Substitutes. Organic & Medicinal Chem IJ. 2020; 10(2): 555782. DOI: 10.19080/OMCIJ.2020.09.555782

In vitro analyses

The cytotoxicity assay is the first step to prove the biocompatibility of a new bone substitute. An ideal response should demonstrate cell viability of 70% or more [11,34]. In Figure 6 is demonstrated the % of cell viability for 75%HAp/25%SF, pressed at 50 MPa and 100 MPa. Alumina was used as a negative control (nontoxic) and phenol as a positive control (toxic). Our composite showed similar behavior to the negative control (Alumina), showing % of cell viability above 80% and no toxicity for CHO cells. We only found toxicity in the positive control (phenol), as was expected. To investigate the bioactivity of our composite, we analyzed the ability to form apatite, a thin layer rich in Ca and P, on the scaffold surface [12,15]. Biomineralization of apatite on the surface of bioactive scaffolds simulates the real reaction between the implanted material and the plasma and other biofluids [35,36]. SEM images (at day 0,14 and 28) for the 75%HAp/25%SF pressed at 50MPa are demonstrated in Figure 7.

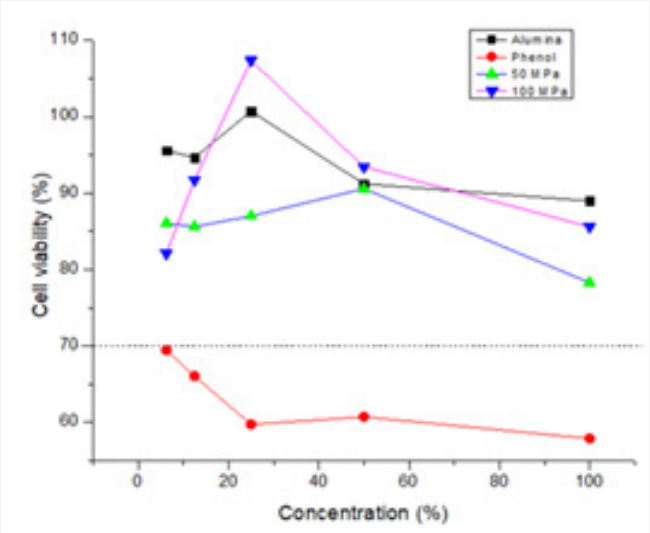

Figure 6: % of cell viability in contact to 75%HAp/25%SF composite, alumina (negative control) and phenol (positive control).

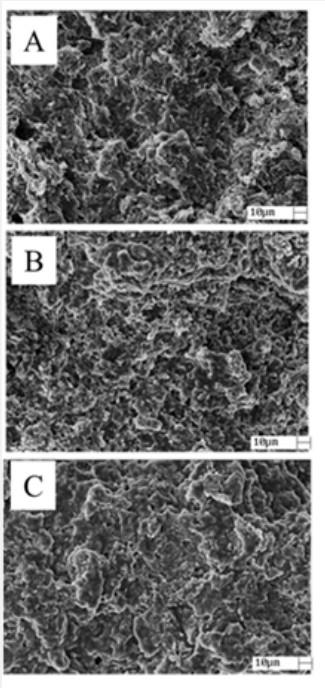

Figure 7: Bioactivity of 75%HAp/25%SF composite showing the apatite growth on scaffold surface at (A) day 0, (B) day 14 and (C) day 28.

How to cite this article: Daniela V, Dayane D, Eliana C d S R, Sheyla M C M B, Sergio A Y. A New Approach to Design Hydroxyapatite and Silk Fibroin Bone Substitutes. Organic & Medicinal Chem IJ. 2020; 10(2): 555782. DOI: 10.19080/OMCIJ.2020.09.555782

Clearly, we can see changes in the morphology at day 14 and 28. In 14 days it is possible to observe a thin layer of apatite growing on the scaffold surface, and more evident at day 28. This result showed the higher bioactivity of 75%HAp/25%SF composite to assist the integration of the implanted material, the new bone and the host tissue when simulating the body environment (SBF solution at 37°C and pH 7.4).

Conclusion

We successful developed a new approach to co-precipitate HAp and SF forming a well homogeneous composite. We studied two different pressures to assemble the scaffold, but no significant differences were found, showing similar behavior for samples framed at 50MPa and 100MPa. The chemical and physical characterizations demonstrated an ideal set of characteristics, such as porosity and mechanical strength. In addition, the final composite presented amorphous structure and inorganic/organic ratio like the trabecular bone. Our results showed an interconnected porous structure allowing the cells, nutrients, and oxygen flows. The designed co-precipitation method is sustainable, simple and cost-effectiveness, without the need of high temperatures, and aggregates values to the discarded silkworm cocoon.

References

1. B B Mandal, A Grinberg, E S Gil, B Panilaitis, D L Kaplan (2012) High-strength silk protein scaffolds for bone repair. Proc Natl Acad Sci 109: 7699.
2. S L McNamara, J Rnjak Kovacina, D F Schmidt, T J Lo, D L Kaplan (2014) Silk as a biocohesive sacrificial binder in the fabrication of hydroxyapatite load bearing scaffolds. Biomaterials 35: 6941.
3. J Melke, S Midha, S Ghosh, K Ito, S Hofmann (2016) Silk fibroin as biomaterial for bone tissue engineering. Acta Biomater 31: 1-16.
4. M M Stevens (2008) Biomaterials for bone tissue engineering. Mater Today 11: 18-25.
5. S Chun, D Yang, S Kim (2012) Comparison study of porous calcium phosphate blocks prepared by piston and screw type extruders for bone scaffold. Tissue Eng Regen Med 9: 51.
6. F Judas, P Palma, R I Falacho, H Figueiredo (2012) Structure and dynamics of bone tissue 1-51.
7. J Jiang, W Hao, Y Li, J Yao, Z Shao, H Li, et al. (2013) Hydroxyapatite/regenerated silk fibroin scaffold-enhanced osteoinductivity and osteoconductivity of bone marrow-derived mesenchymal stromal cells. Biotechnol Lett 35: 657-661.
8. D N Rockwood, R C Preda, T Yücel, X Wang, M L Lovett, et al. (2011) Materials fabrication from Bombyx mori silk fibroin. Nat Protoc 6: 1612.
9. A Ajisawa (2001) Dissolution of silk fibroin with calciumchloride/ethanol aqueous solution [1998]. J Sericultural Sci Jpn 67: 91.
10. ABNT Catalogo 5017.
11. R F Wallin, E F Arscott (1998) Med Device Diagn Ind 20: 96.
12. ABNT Catalogo 23317.
13. L Liu, J Liu, M Wang, S Min, Y Cai, et al. (2008) Preparation and characterization of nano-hydroxyapatite/silk fibroin porous scaffolds. Biomater Sci Polym 19: 325.
14. H J Park, O J Lee, M C Lee, B M Moon, H W Ju, et al. (2015) Fabrication of 3D porous silk scaffolds by particulate (salt/sucrose) leaching for bone tissue reconstruction. Int J Biol Macromol 78: 215-223.
15. A Teimouri, M Azadi, R Emadi, J Lari, A N Chermahini (2015) β-Chitin/gelatin/nanohydroxyapatite composite scaffold prepared through freeze-drying method for tissue engineering applications. Polym Degrad Stab 121: 18.
16. S Alonso Sierra, R Velázquez Castillo, B Millán Malo, R Nava, L Bucio (2017) Interconnected porosity analysis by 3D X-ray microtomography and mechanical behavior of biomimetic organic-inorganic composite materials. Mater Sci Eng 80: 45.
17. L Wang, R Nemoto, M Senna (2004) Changes in microstructure and physico-chemical properties of hydroxyapatite–silk fibroin nanocomposite with varying silk fibroin content. J Eur Ceram Soc 24: 2707.
18. C Fan, J Li, G Xu, H He, X Ye, et al. (2010) Facile fabrication of nano-hydroxyapatite/silk fibroin composite via a simplified coprecipitation route. J Mater Sci 45: 5814-5819.
19. N A Zakharov, L I Demina, A D Aliev, M R Kiselev, V V Matveev, et al. (2017) Synthesis and properties of calcium hydroxyapatite/silk fibroin organomineral composites. Inorg Mater 53: 333.
20. C Du, J Jin, Y Li, X Kong, K Wei, et al. (2009) Novel silk fibroin/hydroxyapatite composite films: Structure and properties. Mater Sci Eng C 29: 62-68.
21. H Zhang, J Magoshi, M Becker, J Y Chen, R Matsunaga (2002) Thermal properties of Bombyx mori silk fibers. J Appl Polym Sci 86: 1817.
22. A Rapacz Kmita, C Paluszkiewicz, A Ślósarczyk, Z Paszkiewicz (2005) FTIR and XRD investigations on the thermal stability of hydroxyapatite during hot pressing and pressureless sintering processes. J Mol Struct 744: 653.
23. A Ślósarczyk, Z Paszkiewicz, C Paluszkiewicz (2005) FTIR and XRD evaluation of carbonated hydroxyapatite powders synthesized by wet methods. J Mol Struct 744: 657.
24. I Mobasherpour, M S Heshajin, A Kazemzadeh, M Zakeri (2007) Synthesis of nanocrystalline hydroxyapatite by using precipitation method. J Alloys Compd 430: 330.
25. X Chen, D P Knight, Z Shao, F Vollrath (2001) Regenerated Bombyx silk solutions studied with rheometry and FTIR. Polymer 42: 09969-09974.
26. S Hofmann, C W P Foo, F Rossetti, M Textor, G Vunjak Novakovic, et al. (2006) Silk fibroin as an organic polymer for controlled drug delivery. J Controlled Release 111: 219.
27. R Nazarov, H J Jin, D L Kaplan (2004) Porous 3-D scaffolds from regenerated silk fibroin. Biomacromolecules 5: 718-726.
28. S Koutsopoulos (2002) Synthesis and characterization of hydroxyapatite crystals: A review study on the analytical methods. J Biomed Mater Res Off J Soc Biomater Jpn Soc Biomater Aust Soc Biomater Korean Soc Biomater 62: 600.
29. R K Brundavanam, G E J Poinern, D Fawcett (2013) Synthesis of a bone like composite material derived from waste pearl oyster shells for potential bone tissue bioengineering applications. Am J Mater Sci 3: 84.
30. R Murugan, S Ramakrishna (2004) Bioresorbable composite bone paste using polysaccharide based nano hydroxyapatite. Biomaterials 25: 3829.
31. E S Gil, J A Kluge, D N Rockwood, R Rajkhowa, L Wang, et al. (2011) Mechanical improvements to reinforced porous silk scaffolds J Biomed Mater Res A 99: 16.

How to cite this article: Daniela V, Dayane D, Eliana C d S R, Sheyla M C M B, Sergio A Y. A New Approach to Design Hydroxyapatite and Silk Fibroin Bone Substitutes. Organic & Medicinal Chem IJ. 2020; 10(2): 555782. DOI: 10.19080/OMCIJ.2020.09.555782

32. X N Qi, Z L Mou, J Zhang, Z Q Zhang (2013) Journal of biomedical materials research. Part A. J Biomed Mater Res Part Off J Soc Biomater Jpn Soc Biomater Aust Soc Biomater Korean Soc Biomater.

33. E Charriere, J Lemaitre, P (2003) Zysset Hydroxyapatite cement scaffolds with controlled macroporosity: fabrication protocol and mechanical properties Biomaterials 24: 809.

34. S O Rogero, A B Lugão, T I Ikeda, Á S Cruz (2003) Teste in vitro de citotoxicidade: estudo comparativo entre duas metodologias. Mater Res 6: 317.

35. H M Kim, T Himeno, M Kawashita, T Kokubo, T Nakamura (2004) The mechanism of biomineralization of bone-like apatite on synthetic hydroxyapatite: an in vitro assessment. J R Soc Interface 1: 17.

36. T Kokubo, H Takadama (2006) How useful is SBF in predicting in vivo bone bioactivity? Biomaterials 27: 2907.

DOI: 10.19080/OMCIJ.2020.10.555782

How to cite this article: Daniela V, Dayane D, Eliana C d S R, Sheyla M C M B, Sergio A Y. A New Approach to Design Hydroxyapatite and Silk Fibroin Bone Substitutes. Organic & Medicinal Chem IJ. 2020; 10(2): 555782. DOI: 10.19080/OMCIJ.2020.09.555782